ADVANCED HEALTHCARE MATERIALS
www.advhealthmat.de

In Situ Nucleic Acid Amplification and Ultrasensitive Colorimetric Readout in a Paper-Based Analytical Device Using Silver Nanoplates

Akkapol Suea-Ngam, Ilada Choopara, Shangkun Li, Mathias Schmelcher, Naraporn Somboonna, Philip D. Howes, and Andrew J. deMello**

A rapid, highly sensitive, and quantitative colorimetric paper-based analytical device (PAD) based on silver nanoplates (AgNPls) and loop-mediated isothermal amplification (LAMP) is presented. It is shown that cauliflower-like concatemer LAMP products can mediate crystal etching of AgNPls, with a threefold signal enhancement versus linear dsDNA. Methicillin-resistant *Staphylococcus aureus* (MRSA), an antimicrobial resistant bacterium that poses a formidable risk with persistently high mortality, is used as a model pathogen. Due to the excellent color contrast provided by AgNPls, the PAD allows qualitative analysis by the naked eye and quantitative analysis using a smartphone camera, with detection limits down to a single copy in just 30 min, and a linear response from 1 to 10^4 copies ($R^2 = 0.994$). The entire assay runs in situ on the paper surface, which drastically simplifies operation of the device. This is the first demonstration of single copy detection using a colorimetric readout, and the developed PAD shows great promise for translation into an ultrasensitive gene-based point-of-care test for any infectious disease target, via modification of the LAMP primer set.

1. Introduction

Effective diagnostic tools are imperative in limiting the spread of infectious diseases.[1] Targeting the genetic material of pathogens in clinical samples using nucleic acid amplification tests (NAATs) allows for versatile and rapid diagnostics that can be readily adapted to new targets, for example during epidemic and pandemic scenarios.[2] Although transferring NAATs from specialized labs to point-of-care environments is an ongoing challenge,[3] diagnostic devices that can be easily read using a mobile device (such as a smartphone or tablet) show great promise.[4] Colorimetric test readouts are highly desirable here as they can be analyzed using a camera and standard software,[5] however simple colorimetric sensing mechanisms that are highly sensitive in themselves are often lacking.

NAATs are recognized as desirable alternatives to traditional culture-based assays,[6] but as yet are insufficiently developed as robust POC diagnostics. Amongst isothermal amplification approaches,[7] loop-mediated isothermal amplification (LAMP) has attracted most attention due to its ability to robustly and sensitively amplify specific DNA targets.[8] Although colorimetric LAMP detection has been demonstrated (e.g., using DNA-staining dyes[9]), sensitive and quantitative analysis remains a distinct challenge.

Paper-based analytical devices (PADs) are cost-effective, allow attachment and/or storage of reaction components in the fiber network, and are amenable to production scale-up.[10,11,12] Recently, Henry and co-workers reported a PAD for AMR detection in bacteria-contaminated water, employing the β-lactamase and nitrocefin assay.[13] Although this method is excellent for assessing bacterial activity, it lacks species specificity, which can be critical in treating infections.[14] Targeting genetic material allows for a much greater depth of analysis, therefore NAATs possess huge potential here.

LAMP has recently been combined with PADs for rapid and cost-effective diagnostics. For example, Cooper and co-workers have developed outstanding origami-based PADs allowing the analysis of complex samples such as whole blood and bovine semen.[15,16] The same group has also developed a multiplex lateral flow system using a similar protocol, which shows promise

A. Suea-Ngam, S. Li, Dr. P. D. Howes, Prof. A. J. deMello
Institute for Chemical and Bioengineering
Department of Chemistry and Applied Biosciences
ETH Zürich
Zürich 8093, Switzerland
E-mail: philip.howes@chem.ethz.ch; andrew.demello@chem.ethz.ch
I. Choopara
Program in Biotechnology
Faculty of Science
Chulalongkorn University
Bangkok 10330, Thailand
Dr. M. Schmelcher
Institute of Food, Nutrition and Health
ETH Zürich
Zürich 8092, Switzerland
Dr. N. Somboonna
Department of Microbiology
Faculty of Science
Chulalongkorn University
Bangkok 10330, Thailand
Dr. N. Somboonna
Microbiome Research Unit for Probiotics in Food and Cosmetics
Chulalongkorn University
Bangkok 10330, Thailand
The ORCID identification number(s) for the author(s) of this article can be found under https://doi.org/10.1002/adhm.202001755

DOI: 10.1002/adhm.202001755

for POC testing.[17] However, in situ analysis of LAMP has to date relied on fluorescence detection,[15–18] providing a minimum limit of detection of 10^2 DNA copies.[19] Although readout is relatively simple under a UV lamp, fluorescence detection adds an extra layer of complexity that would be preferable to remove. Thus, colorimetric approaches are preferred. Although a number of colorimetric LAMP assays have been reported, limitations in sensitivity and lack of in situ amplification prevent field-deployable applications.[20,21]

Noble metal nanoparticles exhibit dramatic shifts in plasmonic character, and therefore their color in solution, as a function of particle aggregation or etching. Linking these processes to biologically-related stimuli (e.g., biomolecular binding, pH changes and enzyme-mediated redox reactions)[22] makes them excellent colorimetric biosensors.[23] Further, they are relatively easy to synthesize, can be dressed with a large variety of capping agents and functional groups for bioconjugation, can be stabilized in a wide range of physiological conditions, and can resist non-specific binding.[24] Accordingly, nanoplasmonics has played a key role in the development of PADs for the sensitive colorimetric detection of many different analytes.[25,26] A particular advantage of nanoplasmonics is the ability to tune the colorimetric response to the physiology of the human eye, thus favoring sensitive detection even with a simple visual readout.[27]

Silver nanoparticles exhibit similar chemistry to gold nanoparticles, including strong thiol binding for capping and conjugation control,[28] but possess some key advantages, including a relatively facile size and morphology control using mild and simple chemistry, and silver's lower cost.[29,30] The interaction of silver with DNA has seen various applications, such as silver metallization of DNA for biosensing,[31] silver-induced DNA damage in bacteria,[32] DNA-templated silver nanocluster synthesis[33] and in dsDNA-based silver nanowires.[34] Such studies indicate the promise in developing nanosystems that coemploy nucleic acids and AgNPs.

Antimicrobial resistance (AMR) in bacterial infections kills more than seven hundred thousand people per year; a number predicted to rise to ten million by 2050.[35] Unsurprisingly, The World Health Organization has stressed the importance of controlling infections on the front line through the provision of appropriate in vitro diagnostics for rapid AMR detection.[36] Motivated by this importance, we use methicillin-resistant *Staphylococcus aureus* (MRSA), the most prevalent AMR pathogen,[37] as a model target in the development of our colorimetric PAD.

In this article, we report a new and highly sensitive assay concept and paper-based analytical device, allowing detection of a target gene sequence down to the single copy level. Points of novelty in this work include: 1) The first use of silver nanoplates (AgNPls) for sensitive colorimetric detection of DNA amplicons based on nanocrystal etching, yielding a quantitative response with excellent sensitivity and color contrast. 2) Invention of LAMP-mediated AgNPl etching allowing extremely sensitive detection, down to a single copy, and excellent selectivity against other bacteria. 3) Successful incorporation of this mechanism into a PAD, including the first demonstration of colorimetric LAMP running in situ on the paper, which concurrently increases sensitivity and simplicity of test operation. A qualitative result can be read by the naked eye, while a quantitative result can be simply derived by smartphone image capture and analysis. Overall, the developed paper-based test shows excellent promise as a versatile field-deployable POC test for infectious diseases.

2. Results and Discussion

2.1. Colorimetric Detection Using Silver Nanoplates

We have combined AgNPls with LAMP to realize the sensitive, specific and colorimetric detection of MRSA via the *mecA* gene (**Figure 1**). Although the numerous MRSA strains contain many different genes that confer drug resistance, the *mecA* gene is found in all MRSA strains,[38] and as such was chosen as a marker for MRSA in the current study. AgNPls are highly anisotropic flat nanostructures (Figure 1a),[39] whose solutions exhibit varied colors due to the dependence of the plasmonic peaks (between 350 and 1000 nm)[40] on both particle size and shape. They readily undergo oxidative etching and crystal reformation as a function environmental redox character.[41] These processes result in significant shifts in solution colors. Halides are known to bind to and etch AgNPls, inducing morphological changes,[41] and DNA is known to interact strongly with silver ions and metal surfaces. It has recently been shown that DNA (particularly short poly sequences) can exert morphological control over AgNPls growing from Ag nanoparticle seeds.[42] Given the etching abilities of halides and the potential of DNA to bind and protect Ag facets, we hypothesized that by exposing the AgNPls to halide salts in various concentrations of LAMP DNA product, a ratiometric shift in AgNPl solution color as a function of *mecA* would occur.

The AgNPls used herein are starch-stabilized, appearing blue-purple in aqueous solution (Figure 1b, inset).[43] TEM analysis (Figure 1b) revealed a mixture of truncated triangular and circular plates (42 ± 8.9 nm diameter) and small discs (7.7 ± 3.9 nm diameter). Absorption spectra (**Figure 2**) display a sharp low-intensity peak at 339 nm indicating the presence of plates, and a broad peak at 400 nm corresponding to the presence of smaller nanoplates and/or nanoparticles. A broad peak occurring between 500 and 550 nm corresponds to the in-plane dipole resonance of larger nanoplates, and shifts as a function of vertex sharpness and lateral size.

First, we identified which halide salts yield the greatest plasmonic shift (Figure 2a), finding that NaBr provides the greatest, with solutions changing from blue-purple to yellow. Accordingly, the in-plane dipole resonance peak blue shifts from 550 to 419 nm, indicating a rounding of nanoplate corners and the formation of smaller nanodiscs.[44,45]

2.2. Assay Development

To validate the LAMP reaction for detection of the *mecA* gene, we designed (Table S1, Supporting Information) and optimized (Table S2, Supporting Information) a LAMP primer set using the PCR product obtained from *mecA* amplification as the target (referred to herein as '*mecA* template', see Supporting Information). Gel electrophoresis (Figure S1, Supporting Information) confirmed the synthesis of the LAMP product, with a small amount of product visible even for the single target copy per µL sample. Next, we assessed the effect of preincubating AgNPls with LAMP

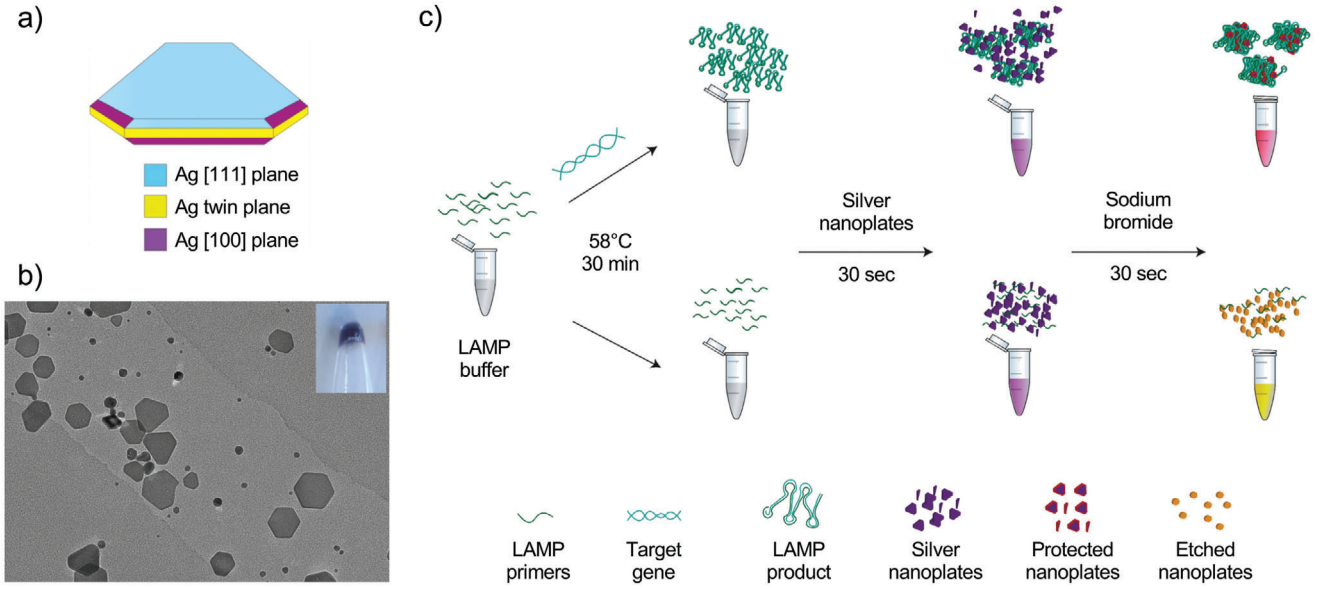

Figure 1. a) Schematic of a silver nanoplate (AgNPl). b) TEM images of the stock AgNPls. c) Colorimetric detection of MRSA using LAMP and AgNPls. In the presence of the target *mecA* gene (top), the LAMP reaction yields a large amount of long DNA concatamer product. Upon addition of a solution of AgNPls, the particles coordinate with the DNA, which then protects them against etching by the subsequently added bromide, and the solution turns red. In contrast, in the absence of the target (bottom), LAMP does not proceed and there is no reaction product to protect the AgNPls from etching, and the reaction solution turns yellow.

products. These amplicons are "cauliflower-like" DNA structures with a range of lengths (up to thousands of bases), comprising a mixture of stem-loops with varied stem lengths.[46] TEM analysis confirmed that the AgNPls were successfully captured by LAMP products (Figure S2a, Supporting Information), resulting in a graying of the blue solution, which is expected given the closer nanoparticle proximity. Capture of AgNPls is explained by the affinity of DNA for Ag surfaces, and the fact that a proportion of the LAMP product is single-stranded (the loop segments), exposing free bases to the Ag. Further, as starch-capped AgNPls are neutral, they do not experience a repulsive force with DNA, in contrast to commonly used citrate-capped Ag nanostructures which are negatively charged at neutral pH.

We next compared solutions of AgNPls with and without pre-incubation with LAMP product (Figure 2b). Incubation with LAMP product (30 s, followed by addition of NaBr) saw the solution rapidly turn red-purple (Figure 2biii), with TEM indicating dense nanoparticle aggregates (Figure S2b, Supporting Information). Absorption spectra exhibited a slight blue shift of the in-plane dipole resonance (550–520 nm), with the appearance of a 400 nm peak (Figure 2biii), indicating that some etching occurs, rounding nanoplate vertices and reducing lateral size.[40] In contrast, in the absence of the target *mecA* (i.e., where no LAMP product forms), the solution rapidly turned yellow-orange, indicating significant etching. TEM analysis (Figure S2c, Supporting Information) demonstrated a reduction in nanoplate size (36.4 ± 10.7 nm diameter) and number, with a significant background population of very small particles. Etching was accompanied by a significant shift of the in-plane dipole resonance peak to 420 nm (Figure 2biv). We therefore conclude that LAMP product inhibits the etching of the AgNPls by bromide. Interestingly, the AgNPls appear to undergo some morphological changes in the presence of only LAMP product under extended incubation (1 h), without the addition of NaBr (Figure S3, Supporting Information). Here, we observe well-rounded, asymmetric nanoplates, with a morphology distinctly different from the parent stock. This concurs with previous studies by Hu et al., who observed poly-C DNA-mediated AgNPl etching and Ostwald ripening.[47] Other studies report that low concentrations of bromide may actually stabilize AgNP [100] facets, but with excess bromide still leading to etching.[48] Accordingly, we note that the mechanism of DNA and bromide stabilization versus etching remains an open question worthy of further attention.

We then assessed LAMP product-mediated etching as a quantitative colorimetric readout for *mecA* by studying AgNPl response across a range of LAMP product concentrations (100–1200 ng). Absorption spectra (**Figure 3**a) indicate nanoplate etching through a gradual blue shift of the in-plane dipole resonance peak and a concurrent increase in the 400 nm plasmon peak, as a function of decreasing LAMP product, which is consistent with our observation that it protects the AgNPls. The signal at 260 nm originates from the LAMP DNA. The LAMP product concentration series data were quantified by two methods (Figure 3b). First, by absorbance at 520 nm (A_{520}). Second, by photographing samples using a smartphone camera, applying a filter to isolate the red channel, converting the images to grayscale and then extracting the grayscale intensity. Figure 3b reveals a linear relationship for both approaches (R^2 = 0.984 for A_{520} and R^2 = 0.992 for grayscale).

Next, to test the full assay concept, a concentration series of the *mecA* template (10–10^{10} ag μL^{-1}, or 1–10^9 copies μL^{-1}) and a negative control were amplified by LAMP and assayed using AgNPls. The process is summarized in Figure 1c. The data in Figure 3c (red line) highlight the linear relationship between the

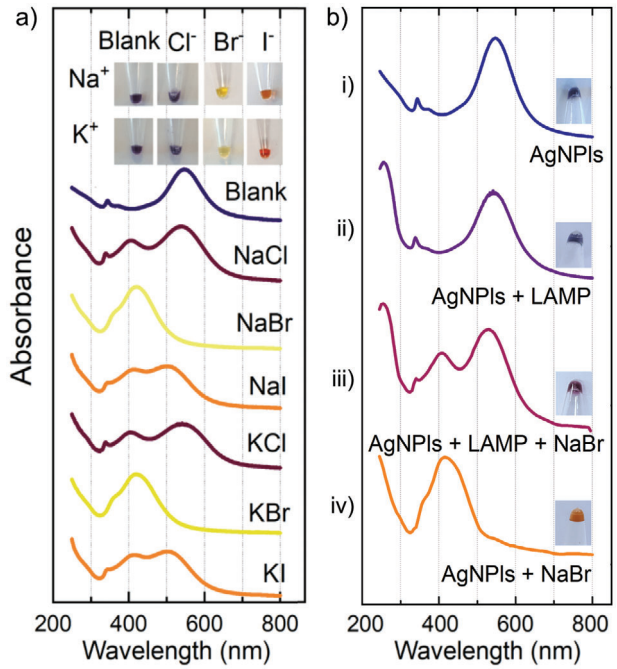

Figure 2. a) AgNPl absorption spectra when incubated with different halide salts. b) The degree of AgNPl etching, and solution color, changes in the presence of the different reaction components, revealing the protective effect that the LAMP product has against etching, and the promise of this mechanism for nucleic acid detection.

grayscale intensity and the log target concentration ($R^2 = 0.994$) across the entire range. Importantly, the excellent sensitivity of LAMP and the sensitive concentration-dependent AgNPl etching allowed for detection even down to a single copy of the target, with an easily readable colorimetric output. We note that, in the initial optimization of the LAMP primers and reaction conditions (Tables S1 and S2, Supporting Information), the small amount of reaction product from the single copy sample was not detectable within the real-time PCR machine, but only after multiple stainings of the agarose gel (Figure S1, Supporting Information). This highlights the excellent sensitivity of the AgNPl mechanism described herein, and is a highly significant result, as it moves ultrasensitive nucleic acid assays away from a reliance on fluorescence for signal transduction, opening the door for a far simpler readout at the point-of-care, for example using smartphone image analysis,[4,5] whilst maintaining the ability for highly accurate quantitation when required.

2.3. Comparison between LAMP and PCR

Next, we investigated whether the AgNPls could interact with PCR products in a similar manner. Following an identical protocol, a similar colorimetric response was observed but with a limit of detection of 10^2 copies (10^3 ag μL^{-1}, compared to 10 ag μL^{-1} (1 copy), for LAMP) and linearity up to 10^7 copies (Figure 3c). These results indicate that the AgNPls interact with the PCR product DNA (Figure S4, Supporting Information), and that this can mediate etching by bromide, but that the structure of the LAMP product favors the protective effect of DNA against etching. For an identical target concentration of 10^3 ag μL^{-1}, PCR yielded 2 µg DNA product in 2 h, while LAMP yielded 700 ng product in 30 min. Nevertheless, the assay response at 10^3 ag μL^{-1} is significantly stronger for LAMP than PCR (Figure 3c). The final assay then achieves a two-orders-of-magnitude better sensitivity with LAMP than with PCR, even with 90 min less incubation time (Figure 3c). We believe that the improved performance of LAMP versus PCR arises due to differences in amplicon structure. LAMP products are hundreds to thousands of bases in length, with a mixture of double-stranded stems and single-stranded loops. In contrast, PCR products are relatively short (685 bases) and double stranded. Accordingly, the lack of unpaired bases in PCR products reduces adsorption to AgNPls and protection against incoming bromide ions. Conversely, the much larger LAMP products form globule-like structures (Figures S2 and S3, Supporting Information), in which the AgNPls are embedded, increasing protection.

2.4. Sample Testing and Specificity Study

Next, we tested the assay directly using lysate from bacterial colonies. Briefly, colonies were collected and lysed in TE buffer at 95 °C for 5 min, then 1 µL of the lysate was added to the assay working solutions before proceeding with the amplification reaction and readout. For both the LAMP and PCR test, red solutions were observed for MRSA, confirming a positive result for *mecA*. The selectivity for MRSA was assessed against other bacterial genera and human pathogens (*Escherichia coli*, *Enterococcus faecalis*, *Staphylococcus epidermidis*, and methicillin-sensitive *S. aureus* (MSSA)). Using PCR and LAMP with subsequent AgNPl incubation (Figure 3d), yellow solutions were observed for all interferent bacteria (indicating no amplification), confirming excellent selectivity for *mecA*.

Finally, detection accuracy was tested using a concentration series of *mecA* template between 10^3 and 10^5 ag μL^{-1}. Three samples were assayed via LAMP and PCR, using the assay test plots (Figure 3c) as calibration curves. The LAMP reaction slightly overestimates *mecA* concentration (Figure S5, Supporting Information), however the %*RSD* for 10^3, 10^4, and 10^5 ag μL^{-1} of target DNA were only 3.6%, 4.2%, and 5.5%, while the %*recovery* at each concentration was 109%, 109%, and 114%, respectively. Compared to PCR, a paired *t*-test indicates no significant difference between the results ($t_{calulated} = 0.003$ and $t_{critical} = 2.14$, $N = 15$).

2.5. Paper-Based Device Integration

Having established the utility of the combined LAMP and AgNPl assay for sensitive detection of MRSA in a tube assay, we next sought to transfer this mechanism onto a PAD to produce a POC-viable diagnostic concept. The LAMP reaction used herein uses six primers (Table S1, Supporting Information). We immobilized one of the loop-forming primers, and therefore the resultant LAMP product, onto the paper surface. Immobilization of the primer was performed by binding streptavidin on cellulose via EDC/NHS coupling, followed by addition of the biotin-modified primer. To evaluate the effect of primer immobilization and confinement of the reaction, a direct comparison

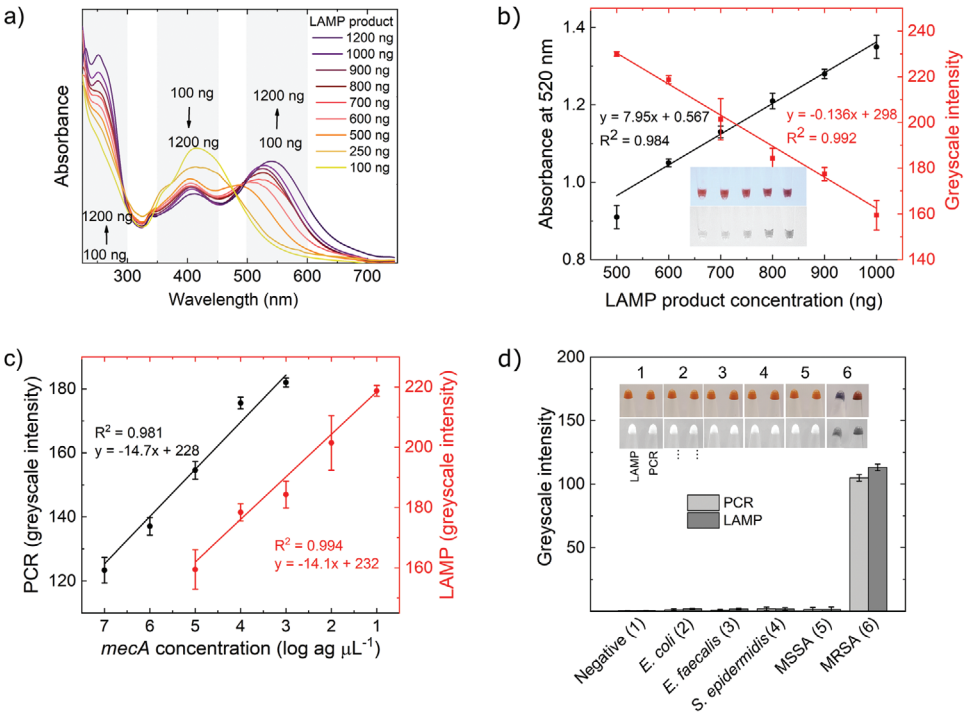

Figure 3. a) Absorption spectra at various LAMP product concentrations, revealing that degree of etching is concentration dependent. b) Calibration curves from absorbance at 520 nm and colorimetric analysis (greyscale intensity) (N = 3). Inset: the corresponding reaction solutions. c) The full assay dose-response curves, comparing PCR and LAMP product performance for the AgNPl assay (N = 3). d) Specificity for MRSA versus other bacteria, for the PCR and LAMP assays (N = 3).

was made between the immobilized and non-immobilized cases (**Figure 4**a). It was found that by immobilizing the FIP primer (Figure S6, see varied immobilized primer study in the Supporting Information), the AgNPls were less etched (i.e., redder), compared to the free primers (orange-yellow in color). The twofold increase in acquired signal suggests that the concentration of LAMP product in the surface layer was higher in the immobilized case, leading to a greater sensitivity.

Next, we developed a PAD to run the assay, as illustrated in Figure 4b. It comprises five layers. Layers one and five are adhesive tape, used to prevent water evaporation, while layers two and four are punched-hole double-sided tape used to space the adhesive tape and the reaction solution. The central layer is a wax-patterned cellulose paper strip with FIP primers immobilized in each reaction well. This approach represents a simple and cost-effective solution to perform a sophisticated amplification reaction on paper.

The paper-based test, illustrated in Figure 4b, is conducted as follows: First, the LAMP primer solution (minus the FIP) is deposited on the paper, followed by a solution containing the target DNA, LAMP buffer, and the polymerase. The whole device is heated to 58 °C (on a hot plate, or in an oven) for 30 min, then the LAMP reaction proceeds in situ in the device. Next, AgNPls are added (30 s incubation), followed by a NaBr solution to develop the color (<30 s). For a positive result, the reaction chamber becomes red. For a negative result, it becomes yellow. Finally, the PAD is photographed (in our case, using a smartphone), the red channel isolated and converted to grayscale, and the grayscale intensity used to quantify the LAMP product. Importantly, each device contains a well for the negative and positive control, meaning that changes in environmental lighting conditions can be corrected for in the image analysis process.

Quantitative analysis of both tube- and paper-based tests was performed using a concentration series of *mecA* template (10–10^{10} ag µL^{-1}, 1–10^{9} copies) to ascertain whether immobilization primer/product and the AgNPl reaction had any deleterious effect. Figure 4c shows a linear relationship from 10 to 10^{5} ag µL^{-1} ($R^2_{\text{tube}} = 0.987$, $R^2_{\text{PAD}} = 0.994$). Due to the excellent sensitivity of the LAMP reaction and the concentration dependent etching of the AgNPls, we could obtain single-copy detection of the target with a colorimetric output. Further, given the comparable data for the tube- versus paper-based approach, there appears to be no detrimental effect of immobilizing the primer/product and AgNPl reaction on the paper.

As before, selectivity for MRSA was tested against other regularly found bacteria (**Figure 5**a) using sample lysates. Yellow (i.e., etched AgNPls) was observed for all of the interferent bacteria, suggesting no amplification product. Red was observed for MRSA, demonstrating that the excellent selectivity for the *mecA* gene was preserved in the paper-based test format. An accuracy test was performed by comparing LAMP for both tube- and paper-based systems directly with PCR, using the AgNPls colorimetric readout. A concentration series of *mecA* template (10^3, 10^4, and 10^5 ag µL^{-1}) was analyzed using the tube- and paper-based LAMP, and tube-based PCR reactions (Figure 5b). The results exhibited excellent agreement, ($R^2_{\text{tube}} = 0.958$, $R^2_{\text{PAD}} = 0.956$) with no significant difference by a paired *t*-test ($t_{\text{cal-tube}} = 0.003$ and $t_{\text{cal-PAD}} = 0.028 < t_{\text{critical}} = 2.14$, $N = 15$). Finally, we determined

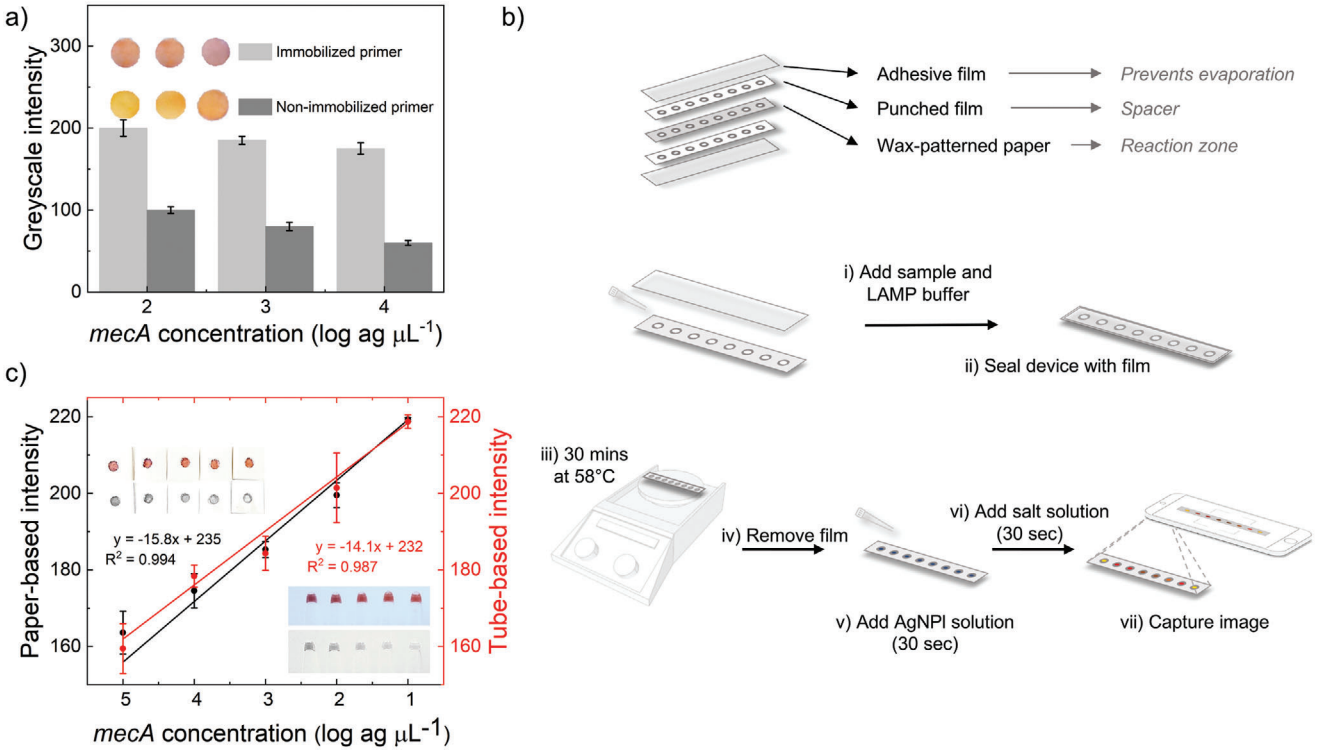

Figure 4. a) Comparing the effect of immobilization versus non-immobilization of the LAMP primer on the cellulose surface, revealing an enhanced signal in the immobilized case (N = 3). b) The PAD device components and test process. After adding the sample and LAMP buffer to the device it is sealed and heated to 58°C for 30 min. A 30 s incubation with added AgNPls, then NaBr, reveals the test result which can then be read by the naked eye (qualitative), or captured by a camera for image analysis (quantitative). c) Direct comparison of the dose–response for the paper-based and tube-based formats, revealing no significant difference in performance (N = 3).

the %*RSD*, and found it to be within an acceptable range (i.e., < 5%) for all concentrations (3.1%, 4.3%, and 3.2% for 10^3, 10^4, and 10^5 ng µL^{-1} of *mecA*, respectively, with $N = 5$).

Finally, the PAD stability over 28 days was studied using the same concentration series as the accuracy tests (Figure S7, Supporting Information). A set of the PADs was stored (4 °C, N_2), and fresh ones used each time. Setting the first tests at 100% efficiency, the final efficiency after 28 days was ≈95%, based on the signal intensity, showing potential for longer term storage and use. We hypothesize that the slight degradation in performance was attributable to degradation of the DNA, which could be alleviated with better packaging in a dry environment.

3. Conclusions

We demonstrate an ultrasensitive and rapid assay and PAD using the interaction between AgNPls and the globulus LAMP product, for the first time, allowing target-modulated particle etching. Using MRSA as a model target, we demonstrate detection via its *mecA* gene, achieving colorimetric detection even down to the single target copy µL^{-1} level in just 30 min. The interaction of the cauliflower-like LAMP products with AgNPls enhances signal threefold versus PCR, which facilitates the extreme sensitivity of our approach. The developed sensing mechanism harnesses the unique nanoscale properties of AgNPls, yielding qualitative analysis by visual inspection and quantitative analysis through the use of a smartphone camera. Specific advantages include high contrast, a wide colorimetric range, a direct proportionality between the degree of etching and the concentration of DNA and high sensitivity, as AgNPls can be used at much lower concentrations than colorimetric dyes. This assay concept was used as the basis for the development of a paper-based test, where target amplification (by LAMP) and signal transduction (by AgNPls) is performed in situ on paper, with a total reaction time of ≈30 min. Immobilization of the FIP primer confines reaction products to the paper surface and yields a twofold higher sensitivity when compared to the solution-based reaction. The PAD retained the excellent sensitivity and specificity of the tube-based assay, and high accuracy was observed by comparison with the tube-based LAMP and PCR methods.

Regarding the use of the developed PAD in a POC setting, there is a requirement for a degree of liquid handling (e.g., sample preparation, master mix and sample mixing, addition to PAD, addition of salt and AgNPls solutions), and a heating step (to 58 °C during incubation). Although these steps are relatively simple to execute, they would preclude use by a completely untrained user. That said, we feel that the platform as developed could be used in a low resource setting by a trained user, and with appropriate and realistic development (e.g., simplified sample preparation,[49,50] or immobilization of further assay components on paper[51]), it could become and widely deployable POC device. Further, having demonstrated that our simple but extremely effective colorimetric sensing using AgNPl etching with PCR and LAMP, we feel that the same approach could be adapted

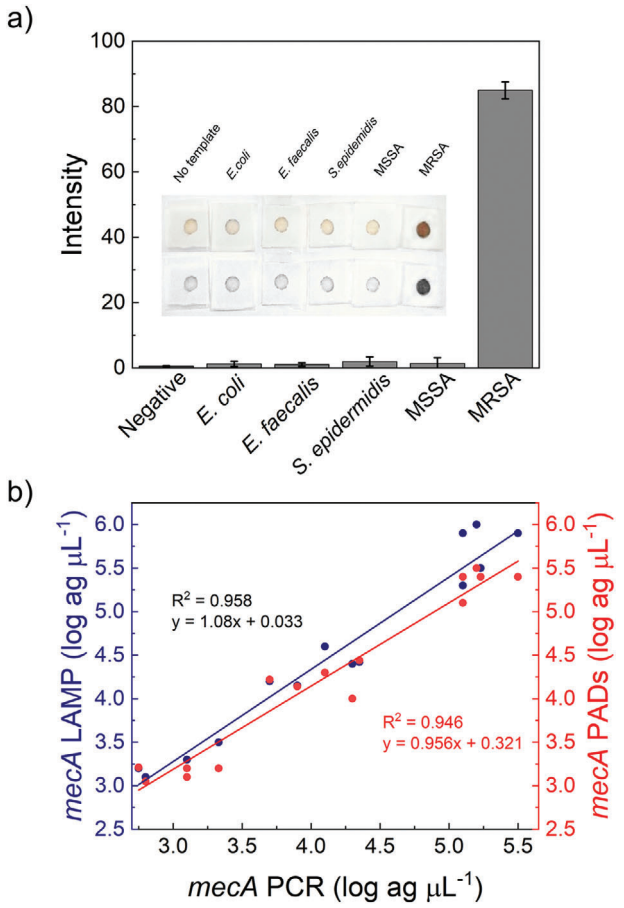

Figure 5. a) Specificity test for MRSA versus other bacteria for the paper-based test, revealing excellent specificity (N = 3). Inset: Raw (upper) and processed images (lower) of the devices. b) Accuracy test for the tube (left axis) and paper-based (right axis) assay formats, revealing excellent correlation with the PCR (bottom axis).

to other nucleic acid amplification approaches, and could therefore achieve widespread uptake and impact in the field of paper-based nucleic acid diagnostics.

This novel device shows promise for the simple and rapid detection of infectious pathogens in a field setting. Rapid adaptation of our approach would allow targeting of a large range of infectious diseases (by redesigning the LAMP primers), and should facilitate sensitive colorimetric detection when used with other nucleic acid amplifications methods.

Supporting Information

Supporting Information is available from the Wiley Online Library or from the author.

Acknowledgements

A.S.N. thanks the State Secretariat for Education, Research and Innovation (SERI) for a Swiss Government Excellence Scholarship (ESKAS No. 2016.0728), Prime Nanotechnology (Bangkok, Thailand) for gifting the Ag-NPls, and Ms. Tamara Zünd for rechecking data. The authors acknowledge ETH ScopeM for technical assistance, and ETH Zurich for partial financial support.

Conflict of Interest

The authors declare no conflict of interest.

Keywords

colorimetric, LAMP, MRSA, paper-based analytical devices, silver nanoplates

Received: October 6, 2020
Revised: November 4, 2020
Published online: November 30, 2020

[1] K. J. Land, D. I. Boeras, X.-S. Chen, A. R. Ramsay, R. W. Peeling, *Nat. Microbiol.* **2019**, *4*, 46.
[2] C. D. Kelly-Cirino, J. Nkengasong, H. Kettler, I. Tongio, F. Gay-Andrieu, C. Escadafal, P. Piot, R. W. Peeling, R. Gadde, C. Boehme, *BMJ Global Health* **2019**, *4*, e001179.
[3] N. Kaur, B. J. Toley, *Analyst* **2018**, *143*, 2213.
[4] C. S. Wood, M. R. Thomas, J. Budd, T. P. Mashamba-Thompson, K. Herbst, D. Pillay, R. W. Peeling, A. M. Johnson, R. A. McKendry, M. M. Stevens, *Nature* **2019**, *566*, 467.
[5] Y. Soda, E. Bakker, *ACS Sens.* **2019**, *4*, 3093.
[6] A. van Belkum, O. Rochas, *Front. Microbiol.* **2018**, *9*, 1437.
[7] Y. Zhao, F. Chen, Q. Li, L. Wang, C. Fan, *Chem. Rev.* **2015**, *115*, 12491.
[8] L. Becherer, N. Borst, M. Bakheit, S. Frischmann, R. Zengerle, F. Von Stetten, *Anal. Methods* **2020**, *12*, 717.
[9] R. Rivero, M. Bisio, E. B. Velázquez, M. I. Esteva, K. Scollo, N. L. González, J. Altcheh, A. M. Ruiz, *Diagn. Microbiol. Infect. Dis.* **2017**, *89*, 26.
[10] D. M. Cate, J. A. Adkins, J. Mettakoonpitak, C. S. Henry, *Anal. Chem.* **2015**, *87*, 19.
[11] M. M. Gong, D. Sinton, *Chem. Rev.* **2017**, *117*, 8447.
[12] N. Jiang, R. Ahmed, M. Damayantharan, B. Ünal, H. Butt, A. K. Yetisen, *Adv. Healthcare Mater.* **2019**, *8*, 1900244.
[13] K. E. Boehle, J. Gilliland, C. R. Wheeldon, A. Holder, J. A. Adkins, B. J. Geiss, E. P. Ryan, C. S. Henry, *Angew. Chem., Int. Ed.* **2017**, *56*, 6886.
[14] M. H. Kollef, *Clin. Infect. Dis.* **2000**, *31*, S131.
[15] Z. Yang, G. Xu, J. Reboud, S. A. Ali, G. Kaur, J. McGiven, N. Boby, P. K. Gupta, P. Chaudhuri, J. M. Cooper, *ACS Sens.* **2018**, *3*, 403.
[16] G. Xu, D. Nolder, J. Reboud, M. C. Oguike, D. A. van Schalkwyk, C. J. Sutherland, J. M. Cooper, *Angew. Chem., Int. Ed.* **2016**, *55*, 15250.
[17] J. Reboud, G. Xu, A. Garrett, M. Adriko, Z. Yang, E. M. Tukahebwa, C. Rowell, J. M. Cooper, *Proc. Natl. Acad. Sci. USA* **2019**, *116*, 4834.
[18] Y. Seok, H. A. Joung, J. Y. Byun, H. S. Jeon, S. J. Shin, S. Kim, Y. B. Shin, H. S. Han, M. G. Kim, *Theranostics* **2017**, *7*, 2220.
[19] B. Li, X. Zhou, H. Liu, H. Deng, R. Huang, D. Xing, *ACS Appl. Mater. Interfaces* **2018**, *10*, 4494.
[20] S. Roy, N. F. Mohd-Naim, M. Safavieh, M. U. Ahmed, *ACS Sens.* **2017**, *2*, 1713.
[21] I. Hongwarittorrn, N. Chaichanawongsaroj, W. Laiwattanapaisal, *Talanta* **2017**, *175*, 135.
[22] P. D. Howes, S. Rana, M. M. Stevens, P. D. Howes, S. Rana, M. M. Stevens, *Chem. Soc. Rev.* **2014**, *43*, 3835.
[23] X. Ma, S. He, B. Qiu, F. Luo, L. Guo, Z. Lin, *ACS Sens.* **2019**, *4*, 782.
[24] C. Parolo, A. Merkoçi, *Chem. Soc. Rev.* **2013**, *42*, 450.
[25] S. Marquez, E. Morales-Narváez, *Front. Bioeng. Biotechnol.* **2019**, *7*, 69.
[26] L. Zhan, S. Z. Guo, F. Song, Y. Gong, F. Xu, D. R. Boulware, M. C. McAlpine, W. C. W. Chan, J. C. Bischof, *Nano Lett.* **2017**, *17*, 7207.
[27] P. Chen, X. Liu, G. Goyal, N. T. Tran, J. C. Shing Ho, Y. Wang, D. Aili, B. Liedberg, *Anal. Chem.* **2018**, *90*, 4916.

[28] A. Ravindran, P. Chandran, S. S. Khan, *Colloids Surf., B* **2013**, *105*, 342.
[29] M. Sabela, S. Balme, M. Bechelany, J. M. Janot, K. Bisetty, *Adv. Eng. Mater.* **2017**, *19*, 1700270.
[30] Y. Sun, Y. Xia, *Science* **2002**, *298*, 2176.
[31] A. Suea-Ngam, P. D. Howes, C. E. Stanley, A. J. Demello, *ACS Sens.* **2019**, *4*, 1560.
[32] M. Ahamed, M. Karns, M. Goodson, J. Rowe, S. M. Hussain, J. J. Schlager, Y. Hong, *Toxicol. Appl. Pharmacol.* **2008**, *233*, 404.
[33] Y. Chen, M. L. Phipps, J. H. Werner, S. Chakraborty, J. S. Martinez, *Acc. Chem. Res.* **2018**, *51*, 2756.
[34] J. Kondo, Y. Tada, T. Dairaku, Y. Hattori, H. Saneyoshi, A. Ono, Y. Tanaka, *Nat. Chem.* **2017**, *9*, 956.
[35] J. O'Neil, *Tackling drug-resistant infections globally: Final report and recommendations*, HM Government, United Kingdom **2016**. https://amr-review.org/home.html.
[36] WHO, *WHO Competency Framework for Health Workers' Education and Training on Antimicrobial Resistance*, World Health Organization, Geneva **2018**.
[37] N. A. Turner, B. K. Sharma-Kuinkel, S. A. Maskarinec, E. M. Eichenberger, P. P. Shah, M. Carugati, T. L. Holland, V. G. Fowler, *Nat. Rev. Microbiol.* **2019**, *17*, 203.
[38] M. Miragaia, *Front. Microbiol.* **2018**, *9*, 2723.
[39] J. Xia, Z. L. Dong, Y. Cai, G. Guan, S. Zhang, A. Kovács, C. Boothroyd, I. Y. Phang, S. Liu, M. Wu, Y. W. Zhang, X. Hu, M.-Y. Han, *Chem. – Eur. J.* **2018**, *24*, 15589.
[40] M. Rycenga, C. M. Cobley, J. Zeng, W. Li, C. H. Moran, Q. Zhang, D. Qin, Y. Xia, *Chem. Rev.* **2011**, *111*, 3669.
[41] Y. Zheng, J. Zeng, A. Ruditskiy, M. Liu, Y. Xia, *Chem. Mater.* **2014**, *26*, 22.
[42] J. Li, Z. Zhu, F. Liu, B. Zhu, Y. Ma, J. Yan, B. Lin, G. Ke, R. Liu, L. Zhou, S. Tu, C. Yang, *Small* **2016**, *12*, 5449..
[43] T. Parnklang, C. Lertvachirapaiboon, P. Pienpinijtham, K. Wongravee, C. Thammacharoen, S. Ekgasit, *RSC Adv.* **2013**, *3*, 12886.
[44] K. E. Lee, A. V. Hesketh, T. L. Kelly, *Phys. Chem. Chem. Phys.* **2014**, *16*, 12407.
[45] B. Tang, S. Xu, J. An, B. Zhao, W. Xu, J. R. Lombardi, *Phys. Chem. Chem. Phys.* **2009**, *11*, 10286.
[46] T. Notomi, H. Okayama, H. Masubuchi, T. Yonekawa, K. Watanabe, N. Amino, T. Hase, *Nucleic Acids Res.* **2000**, *28*, 63e.
[47] S. Hu, T. Yi, Z. Huang, B. Liu, J. Wang, X. Yi, J. Liu, *Mater. Horiz.* **2019**, *6*, 155.
[48] V. Kitaev, T. Subedi, *Chem. Commun.* **2017**, *53*, 6444.
[49] C. Myhrvold, C. A. Freije, J. S. Gootenberg, O. O. Abudayyeh, H. C. Metsky, A. F. Durbin, M. J. Kellner, A. L. Tan, L. M. Paul, L. A. Parham, K. F. Garcia, K. G. Barnes, B. Chak, A. Mondini, M. L. Nogueira, S. Isren, S. F. Michael, I. Lorenzana, N. L. Yozwiak, B. L. MacInnis, I. Bosch, L. Gehrke, F. Zhang, P. C. Sabeti, *Science* **2018**, *360*, 444.
[50] E. Noviana, S. Jain, J. Hofstetter, B. J. Geiss, D. S. Dandy, C. S. Henry, *Anal. Bioanal. Chem.* **2020**, *412*, 3051.
[51] K. Yamada, H. Shibata, K. Suzuki, D. Citterio, *Lab Chip* **2017**, *17*, 1206.